Meteoritics & Planetary Science 37, 125–141 (2002)
Available online at http://www.uark.edu/meteor

The halite-bearing Zag and Monahans (1998) meteorite breccias: Shock metamorphism, thermal metamorphism and aqueous alteration on the H-chondrite parent body

ALAN E. RUBIN[1]*, MICHAEL E. ZOLENSKY[2] AND ROBERT J. BODNAR[3]

[1]Institute of Geophysics and Planetary Physics, University of California, Los Angeles, California 90095-1567, USA
[2]NASA Johnson Space Center, Mail Stop ST, Houston, Texas 77058, USA
[3]Department of Geological Sciences, Virginia Polytechnic Institute and State University, Blacksburg, Virginia 24061, USA
*Correspondence author's e-mail address: aerubin@ucla.edu

(Received 2001 May 15; accepted in revised form 2001 October 19)

Abstract–Zag and Monahans (1998) are H-chondrite regolith breccias comprised mainly of light-colored metamorphosed clasts, dark clasts that exhibit extensive silicate darkening, and a halite-bearing clastic matrix. These meteorites reflect a complex set of modification processes that occurred on the H-chondrite parent body. The light-colored clasts are thermally metamorphosed H5 and H6 rocks that were fragmented and deposited in the regolith. The dark clasts formed from light-colored clasts during shock events that melted and mobilized a significant fraction of their metallic Fe-Ni and troilite grains. The clastic matrices of these meteorites are rich in solar-wind gases. Parent-body water was required to cause leaching of chondritic minerals and chondrule glass; the fluids became enriched in Na, K, Cl, Br, Al, Ca, Mg and Fe. Evaporation of the fluids caused them to become brines as halides and alkalies became supersaturated; grains of halite (and, in the case of Monahans (1998), halite with sylvite inclusions) precipitated at low temperatures (≤100 °C) in the porous regolith. In both meteorites fluid inclusions were trapped inside the halite crystals. Primary fluid inclusions were trapped in the growing crystals; secondary inclusions formed subsequently from fluid trapped within healed fractures.

INTRODUCTION

Many ordinary chondrites (OC) experienced significant parent-body alteration after agglomerating in the solar nebula. Alteration processes included thermal metamorphism (*e.g.*, Wood, 1962; Van Schmus and Koffman, 1967; Dodd, 1969; McSween *et al.*, 1988), shock metamorphism (*e.g.*, Dodd and Jarosewich, 1979; Stöffler *et al.*, 1991), aqueous alteration (*e.g.*, Hutchison *et al.*, 1987; Zolensky *et al.*, 1999a,b; Grossman *et al.*, 2000), brecciation (*e.g.*, Fredriksson and Keil, 1963; Fodor and Keil, 1976; Rubin *et al.*, 1983), implantation of solar-wind gases (*e.g.*, Konig *et al.*, 1961; Suess *et al.*, 1964; Schultz and Signer, 1977), and lithification by minor impact-induced melting along grain boundaries (Bischoff *et al.*, 1983).

Thermal metamorphic effects included textural recrystallization of chondrules and matrix, devitrification of chondrule glass, growth of plagioclase, Ca-pyroxene and Ca-phosphate, mineral compositional equilibration, and bulk loss of volatile trace elements (*e.g.*, Van Schmus and Wood, 1967; Tandon and Wasson, 1968; Lipschutz and Woolum, 1988).

Shock metamorphic effects included development of undulose extinction, mosaic extinction and planar fractures in silicate minerals, production of metal and sulfide veins, transformation of crystalline plagioclase into maskelynite, the formation of silicate-rich melt pockets, and the production of impact-melt rocks.

Aqueous alteration caused loss of mesostasis (and concomitant depletion of alkalies and Al) in the porous outer zones of radial pyroxene and cryptocrystalline chondrules (Grossman *et al.*, 2000). Other effects included the production in type-3 chondrites of rare phyllosilicates (*e.g.*, Hutchison *et al.*, 1987) and opaque nodules containing Fe sulfide, magnetite, carbide, Ni-rich sulfide, Ni-rich taenite and Co-rich kamacite (Krot *et al.*, 1997; Choi *et al.*, 1998). Recently, millimeter-size aggregates of purple halite (NaCl) containing crystals of sylvite (KCl) and aqueous fluid inclusions were reported in the matrix of Monahans (1998), hereafter Monahans (Zolensky *et al.*, 1999a). Fluid inclusions were reported in Zag halite by Whitby *et al.* (2000) and Bridges and Grady (2000).

Ordinary chondrite parent-body alteration processes were diverse and complex. Detailed study of the few meteorites

Prelude preprint MS#4549

that exhibit diverse alteration effects can potentially shed new light on the relative timing and importance of alteration processes. Such meteorites include Zag and Monahans. Zag fell in August 1998 in Western Sahara; ~175 kg were recovered (Grady, 2000). Monahans fell on 1998 March 22 in the city of Monahans, Texas; two stones (1344 and 1243 g) were recovered (Grady, 2000). Halite was reported in both meteorites soon after their fall (Zolensky *et al.*, 1999a,b).

ANALYTICAL PROCEDURES

A 6.7 kg individual piece of Zag owned by Mr. Edwin Thompson was made available for examination. Denatured alcohol was used as a cooling agent for the saw during initial cutting; this procedure preserved the halite crystals. Thin sections were made of 11 portions (clasts and matrix areas) of Zag with different macroscopic characteristics (Table 1). The material was studied microscopically in transmitted and reflected light. Grain sizes were determined microscopically using a calibrated reticle. Mineral analyses were made with the Cameca "Camebax-microbeam" electron microprobe at the University of California, Los Angeles (UCLA) using natural and synthetic standards, 20 s counting times, and PAP corrections (Cameca's version of ZAF correction procedures).

The first of the two recovered Monahans stones (1243 g) was hand-carried to the Johnson Space Center (JSC) for initial sampling within 50 h of its fall. After the halite was discovered, a thin section was made using only isopropyl alcohol to preserve the halides. All analyses of Monahans were made with a Cameca Camebax electron microprobe at JSC using natural and mineral standards, variable counting times, and PAP corrections. The compositions of halide minerals were determined by electron microprobe analysis using a rastered beam, and employing natural mineral standards for Br and K, and pretzel salt (Snyders of Hanover) for Na and Cl. Measurement errors for the Br are <12% relative. Errors for other elements are <5% relative. The poor totals for the analyses of two of the Monahans halite grains are due in part to fluid inclusions within the halite grains that decrepitated under the electron beam during analysis, enhancing sample instability. Halite from Monahans and Zag are unstable in typical laboratory air, and thus were stored in dry nitrogen.

TABLE 1. Petrologic type and shock stage of Zag clasts and matrix regions.

Dark clasts	Light-colored clasts	Chondrule-free clast	Matrix regions
A1: H5, S5	A4: H6, S4	A3: S2	A7: S2
A2: H5, S4	A5: H5, S2	–	D1: S3
B2: H4, S4	A6: H5, S2	–	–
–	B1: H5, S2	–	–
–	C2: H6, S4	–	–

RESULTS

Petrographic, Mineralogic and Geochemical Characteristics of Zag

Whole-Rock–Zag is a breccia consisting of light-colored metamorphic clasts, dark clasts exhibiting extensive silicate darkening, impact-melt-rock clasts, and clastic matrix material. Many of the individual pieces of Zag exported from Africa consist primarily of light-colored metamorphic clasts (E. Thompson, pers. comm., 2001); relatively few fragments appear to be breccias with diverse lithologies. The 6.7 kg breccia that we studied (Fig. 1a) consists of 45 ± 10 vol% light-colored metamorphic clasts, ~5 vol% dark clasts exhibiting silicate darkening, ≤1 vol% impact-melt-rock clasts, and 50 ± 10 vol% clastic matrix.

Portions of the Zag matrix contain substantial amounts of He^4 ((1192–44 200) × 10^{-8} cm^3 STP/g; Schultz and Franke, 2000) indicating that Zag is a regolith breccia with solar-wind-implanted light noble gases.

Light-Colored Metamorphic Clasts–The light-colored clasts in the 6.7 kg specimen (Fig. 1a) range from 0.1 to 15 cm in maximum dimension and possess subrounded, subangular and angular shapes (following the shape criteria for sedimentary particles; Powers, 1953). The clasts have recrystallized textures and relatively equilibrated olivine and low-Ca pyroxene compositions; no glassy mesostases occur within the chondrules. Five light-colored clasts were studied (Table 1): three are petrologic type 5 and contain readily delineated chondrules; two are type 6 and contain highly recrystallized chondrules integrated with matrix.

Olivine ($Fa_{19.0\pm0.4}$; n = 14), low-Ca pyroxene ($Fs_{16.7\pm0.3}$ $Wo_{1.3\pm0.2}$; n = 13) and plagioclase ($Ab_{80.8\pm1.8}Or_{8.7\pm1.9}$; n = 6) have approximately the same narrow ranges in composition in all of the light-colored clasts (Table 2). These values are within the established ranges of H-group chondrites ($Fa_{17.3–20.2}$; $Fs_{15.7–18.1}$; $Ab_{79.2–82.9}$) (Rubin, 1990; Gomes and Keil, 1980; Van Schmus and Ribbe, 1968). Kamacite contains 6.6 ± 0.3 wt% Ni; rare grains of martensite with 8–11 wt% Ni also occur. Troilite in the clasts is essentially pure FeS with Ni typically below the detection limit of 0.04 wt%; however, some troilite grains have low but measurable concentrations of Ni (0.05–0.06 wt%).

Diverse shock effects are evident in the clasts. The three H5 clasts are shock stage S2 and the two H6 clasts are shock stage S4. The clasts exhibit slight to moderate silicate darkening (Rubin, 1992); they contain curvilinear trails of tiny (0.2–2 μm) blebs of metal and troilite that cut through silicate grains and decorate silicate grain boundaries.

Chromite also exhibits varying degrees of shock. Clast A4 contains fractured chromite, clast C2 contains a few trails of small chromite blebs, and clast B1 contains a 750 × 900 μm inclusion consisting of ~50 vol% chromite clusters (each composed of several 2–20 μm individual chromite grains)

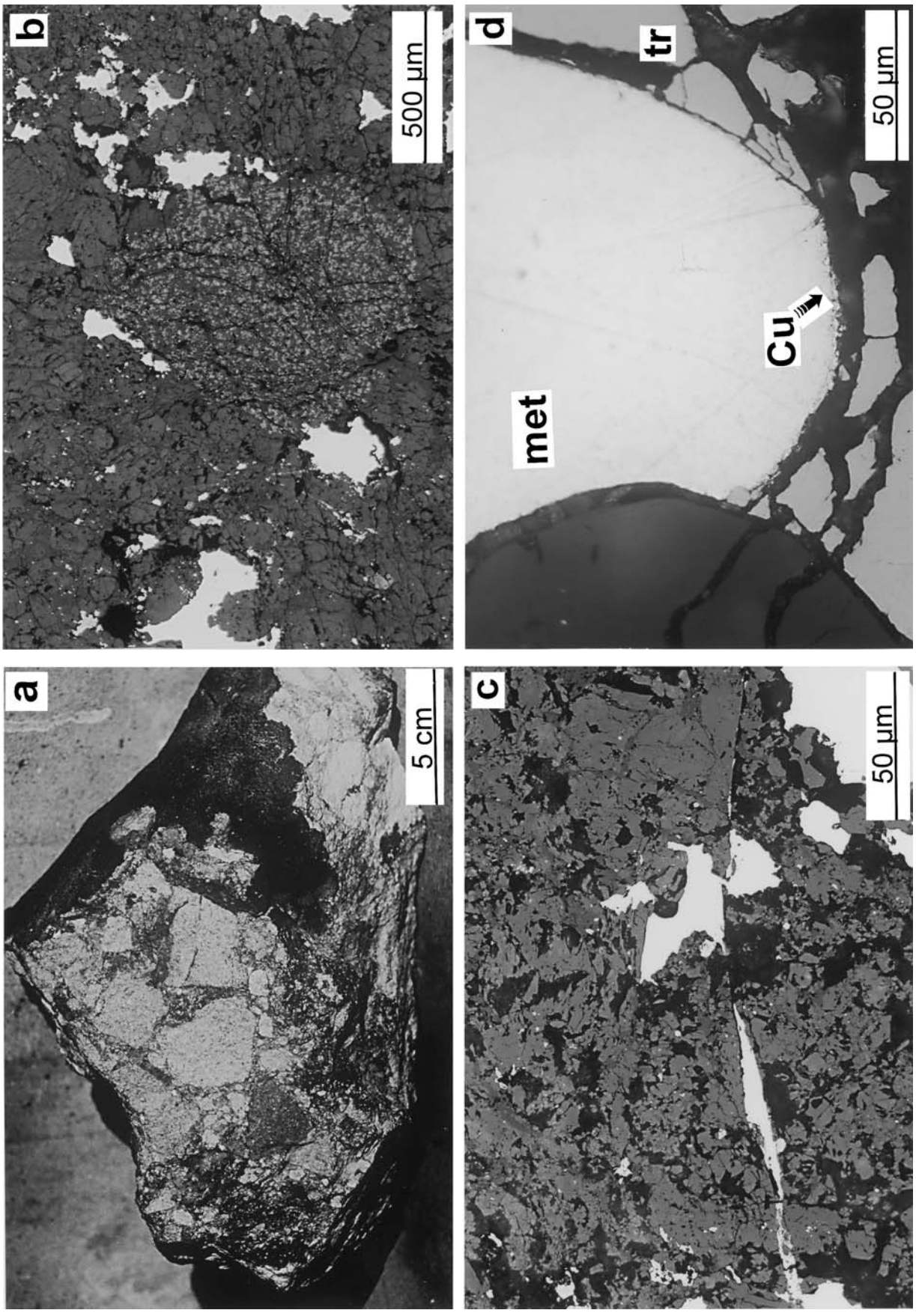

FIG. 1. Zag whole-rock and petrographic characteristics of light-colored metamorphic clasts. (a) The 6.7 kg specimen of Zag from which clasts were removed for this study. The light-colored angular clasts are H5 and H6 chondrite material, the dark gray clasts are silicate-darkened metamorphic clasts, and the gray material between the clasts is the clastic matrix. Some fusion crust (black) is visible at the surface of the specimen. (b) A 750 × 900 μm inclusion in clast B1 consisting of chromite clusters (medium gray) surrounded by plagioclase (dark gray). Reflected light. (c) A sheared or faulted metal grain in clast A6. Reflected light. (d) Ribbon of metallic Cu (light gray) lining the curved interface of metallic Fe-Ni (met = white) and troilite (tr = medium gray) within an opaque assemblage in a light-colored metamorphic clast.

TABLE 2. Mean compositions (wt%) of silicate and oxide minerals in Zag.

	Olivine	Low-Ca pyx	Sub-calcic augite	Diopside	Plagioclase	Chromite*
# grains	20	19	1	1	8	6
SiO_2	38.8 ± 0.6	55.8 ± 0.8	55.0	52.5	65.2 ± 0.8	<0.04
TiO_2	<0.04	0.23 ± 0.11	0.24	0.53	<0.04	2.2 ± 0.3
Al_2O_3	<0.04	0.19 ± 0.10	0.21	0.94	21.3 ± 0.6	6.2 ± 0.2
Cr_2O_3	0.05 ± 0.04	0.21 ± 0.06	0.37	0.91	<0.04	55.8 ± 1.3
FeO	17.7 ± 0.4	11.2 ± 0.2	8.9	3.8	0.58 ± 0.25	27.2 ± 1.3
MnO	0.45 ± 0.05	0.48 ± 0.03	0.39	0.24	<0.04	0.75 ± 0.15
MgO	42.6 ± 0.3	30.8 ± 0.3	26.0	16.8	<0.04	3.9 ± 0.8
CaO	<0.04	0.67 ± 0.11	7.9	22.4	2.1 ± 0.4	<0.04
Na_2O	<0.04	<0.04	0.10	0.50	8.8 ± 0.6	<0.04
K_2O	<0.04	<0.04	<0.04	<0.04	1.4 ± 0.3	<0.04
Total	99.6	99.6	99.1	98.6	99.4	96.0
Fa (mol%)	18.9	–	–	–	–	–
Fs (mol%)	–	16.7	13.6	6.1	–	–
Wo (mol%)	–	1.3	15.5	46.0	–	–
Ab (mol%)	–	–	–	–	80.9	–
Or (mol%)	–	–	–	–	8.5	–

*All oxidized iron expressed as FeO. The low total may indicate that some of the iron is ferric.

embedded in plagioclase (Fig. 1b). The inclusion is similar to chromite-plagioclase patches in Portales Valley (*e.g.*, Fig. 5 of Rubin *et al.*, 2001) and other shocked chondrites.

Some clasts contain veins of metallic Fe-Ni and troilite about 0.02–1 mm thick and about 1–50 mm long. A 5 mm long shock vein in clast A4 has distinct zones: one with massive troilite containing ~2 vol%, ~0.4 μm in diameter metal blebs; another with 2–10 μm silicate grains is surrounded by troilite and contains narrow fractures filled with troilite; a third, metal-rich, zone contains small silicate grains and little troilite; and a fourth zone consists of a fine-grained metal-troilite intergrowth. Clast A6 contains thin metal veins exhibiting preferential orientation; one of these metal grains has a fault or a shear zone (Fig. 1c).

Metallic Cu occurs in some opaque grains at the troilite-metal interface as small (0.5–2 μm) isolated patches, a string of separate irregularly shaped grains, and a curvilinear 1 × 150 μm size ribbon (*e.g.*, Fig. 1d). One metal grain in clast A6 contains thin parallel stringers of troilite intercalated with metallic Cu.

Dark Clasts Exhibiting Silicate Darkening–The dark clasts range from ~0.2 to 5 cm in size and have angular shapes (Fig. 2a). Clasts A1 and A2 are H5 and contain conspicuous chondrule outlines; clast B2 (H4) contains well-defined chondrules. The clasts are all moderately to strongly shocked; many of their olivine grains have mosaic extinction. Rare grains of maskelynite occur in clast A1. All of the clasts exhibit extensive silicate darkening (Fig. 2a). Numerous veinlets of troilite cut through the mafic silicate grains; some of the troilite veinlets contain small patches of chromite. Also present are numerous curvilinear trails of troilite blebs, elongated chromite blebs and narrow chromite veinlets. Some plagioclase patches contain small, nearly equant 2–6 μm size chromite grains. Many chromite grains of typical size (10–20 μm) are cut by troilite veins (Fig. 2b).

The edges of many coarse (100–500 μm) metal grains contain fine-grained troilite-metal cellular and dendritic intergrowths. In clast A1, the distance between the dendrite arms is fairly uniform; ~85% of them are 6 μm. Small (0.5 × 3 μm) metallic Fe-Ni blebs within troilite are elongated and wormy; they are not dendritic (Fig. 2c). The few coarse troilite grains in clast A1 are polycrystalline.

Metallic Cu occurs in clasts A2 and B2 as small grains within metallic Fe-Ni at metal-troilite interfaces. None was observed in clast A1.

Some grains of metallic Fe-Ni in clast A2 contain elongated (and in some cases, stubby) silicate grains arranged in subparallel curved streaks. Some of these metal grains contain coarse troilite that forms a convex interface with the metal (Fig. 2d).

Olivine ($Fa_{18.8\pm0.4}$; n = 6), low-Ca pyroxene ($Fs_{16.7\pm0.3}$ $Wo_{1.2\pm0.1}$; n = 6) and plagioclase ($Ab_{80.4\pm1.2}Or_{7.2\pm1.2}$; n = 4) in the dark clasts are statistically indistinguishable in composition from those in the light-colored clasts. Metallic Fe-Ni consists of kamacite with 6.6 ± 0.4 wt% Ni (n = 9), taenite with ~20 wt% Ni, and rare grains of martensite with ~10 wt% Ni.

Chondrule-Free Clast–Clast A3 contains numerous fine-grained silicate grains (Fig. 3a), a few coarse mafic silicate grains (most likely chondrule fragments) but no intact chondrules. A few large metallic Fe-Ni grains containing shattered silicate grains surrounded by troilite and transected by troilite veinlets also occur (Fig. 3b). Some of the shattered

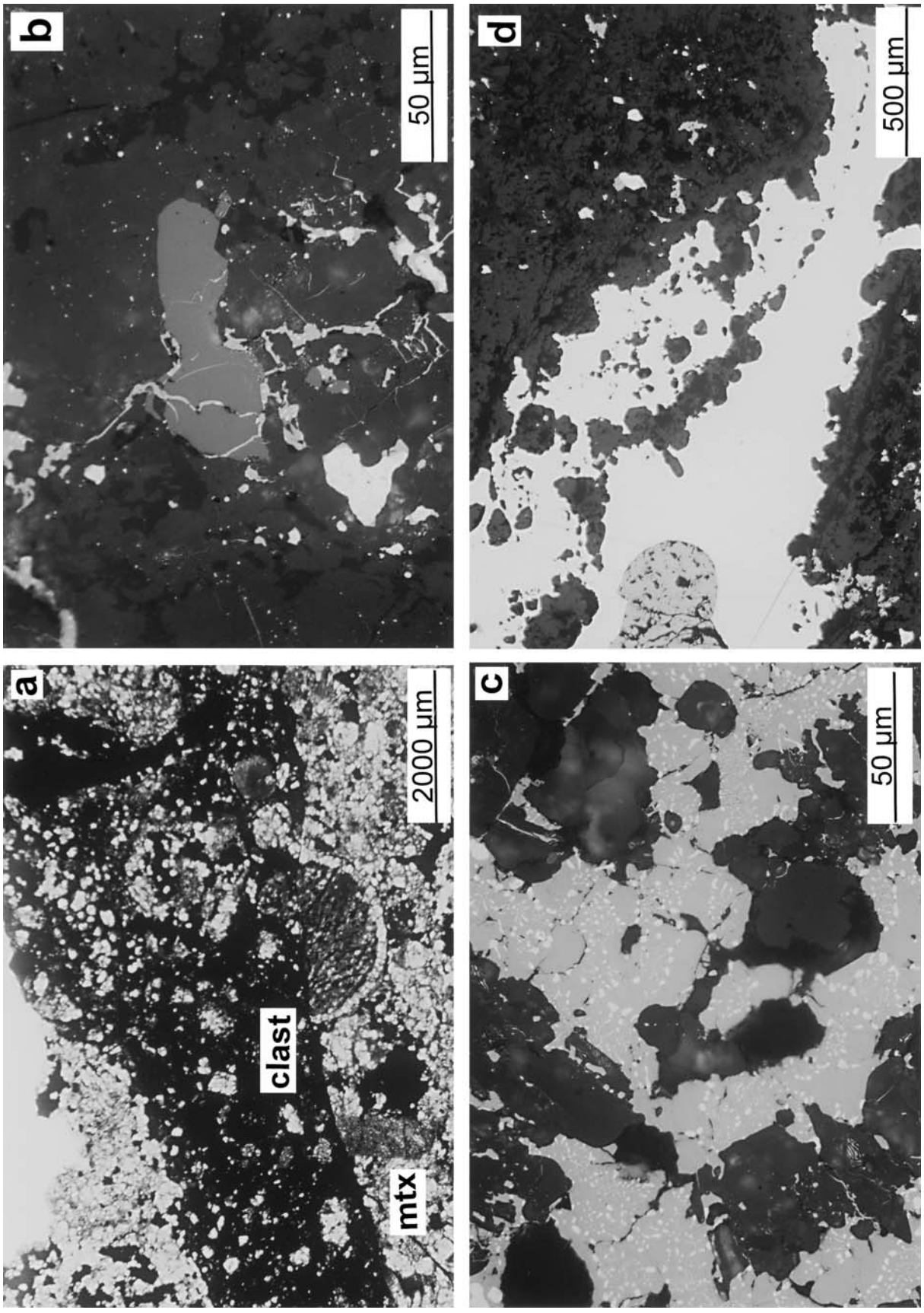

FIG. 2. Petrographic characteristics of dark clasts in Zag. (a) Elongated angular dark clast exhibiting extensive silicate darkening. The surrounding matrix (mtx) is lighter colored and contains discernable chondrules. (b) Typical chromite grain (medium gray) cut by a small troilite vein (light gray). (c) Small wormy metallic Fe-Ni blebs (white) within troilite (medium gray) formed by shock melting and quenching. (d) Metallic Fe-Ni grain (white) with apparently sheared silicate (dark gray). Present at left is a phallic-shaped grain of troilite (medium gray) protruding into the metallic Fe-Ni.

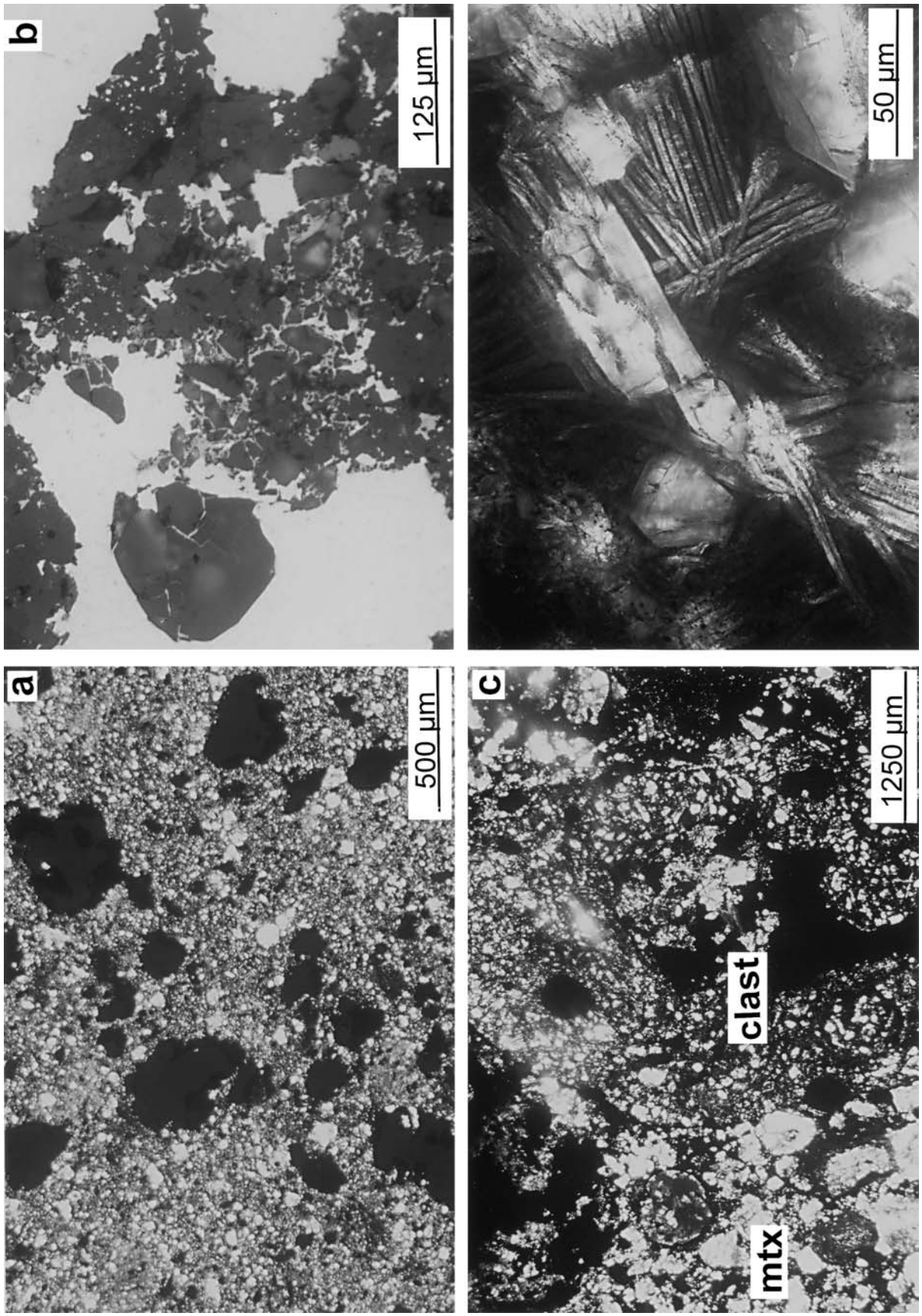

FIG. 3. Impact-melt-rock clasts in Zag. (a) Clast A3 contains abundant fine-grained silicates, but no intact chondrules. Transmitted light. (b) A coarse grain of metallic Fe-Ni (white) in clast A3 containing shattered silicate grains (dark gray) surrounded by troilite (medium gray), transected by troilite veinlets and bridged by patches of troilite. (c) A 5 mm size impact-melt rock clast in matrix (mtx) region D1. (d) Olivine laths within radial clusters in the silicate-melt portion of the melt-rock clast.

1–20 μm size silicate grains occur in clusters that are connected to silicate grains outside of the metal. The silicate grains are bridged by patches of troilite (Fig. 3b). A few small grains of chromite are also present. Elongated, curvilinear (1–2) × (20–30) μm size stringers of troilite occur in some of the coarse metal grains. No coarse, metal-free troilite grains are present in the clast.

The fine-fraction of the clast consists of (a) isolated 0.2–10 μm size irregularly shaped metal grains, (b) metal-sulfide intergrowths (1–10 μm) containing metal spherules rimmed on one side by troilite, (c) small (3–7 μm) chromite grains, (d) rare isolated 3–5 μm size irregular grains of troilite, and (e) small (5–20 μm size) silicate grains. No metallic Cu was observed.

The fine-grained silicates are essentially unstrained; most have sharp to slightly undulose extinction and are of shock stage S1–S2. A few appear recrystallized and resemble the relic mafic silicate clusters in the impact-melted portions of the Rose City and Chico impact-melt breccias (Fig. 1 of Rubin, 1995). Some of the small silicate grains in these clusters exhibit 120° triple junctures; tiny (0.1–0.2 μm size) opaque grains line the boundaries between the fine-grained silicates in the clusters.

Matrix Regions–Matrix regions are those portions of the meteorite located between large clasts. These regions are themselves clastic and contain angular and irregular light-colored metamorphic clasts and dark clasts (Fig. 1a). The clasts in region A7 range in size from a few hundred micrometers to several millimeters. The light-colored clasts in region D1 are H6 clasts ranging in size from 1 to 12 mm. Intermixed in the clastic matrix regions are some recrystallized chondrules, chondrule fragments, and coarse grains of metallic Fe-Ni and sulfide that are not obviously part of larger clasts. Many of the coarse metal grains contain silicate grain fragments.

The clastic matrix exhibits significant silicate darkening; overall, the matrix is appreciably darker than the light-colored metamorphic clasts, but not as dark as the dark clasts. Silicates within the clastic matrix contain short trails of chromite blebs and needles, curvilinear trails of tiny troilite and metal blebs, small metallic Fe-Ni veinlets and millimeter-long veins of metallic Fe-Ni and troilite. Small (2–8 μm size) grains of metallic Cu occur within some of the metallic Fe-Ni grains at the interface with troilite.

Olivine grains in matrix region A7 exhibit undulose extinction (but no planar fractures) characteristic of shock stage S2. In contrast, many olivine grains in region D1 have planar fractures characteristic of shock stage S3.

Region D1 contains a 4.8 × 5.4 mm size impact-melt-rock clast (Fig. 3c). The melt, which constitutes ~75 vol% of the clast, contains faceted 40–130 μm size olivine grains, elongated ((4–8) × (40–80) μm size) olivine laths, and interstitial melt containing abundant tiny (0.3–1.0 μm) opaque blebs. The olivine laths occur as isolated grains and as parts of radial clusters (Fig. 3d). The remaining 25 vol% of the clast consists of metallic Fe-Ni and minor troilite. One large grain is a fine-grained, dendritic intergrowth of metal and troilite. Dendrite spacings near the edge of the clast are 6–8 μm; those near the center of the metal grain average ~14 μm.

In the center of the melt-rock clast is a large (~1180 μm long) unmelted polycrystalline silicate grain containing olivine with mosaic extinction (characteristic of shock stage S4) and exhibiting moderate darkening caused by metal and troilite veinlets and trails of chromite needles. The clast is surrounded by silicate melt and veins of metallic Fe-Ni and troilite.

Halite Grains–The matrix is the only component of the Zag breccia that contains scattered grains of dark blue, transparent to opaque halite (NaCl). Most grains are a few hundred micrometers in size, although aggregates can range up to 1 cm. Sylvite (KCl) was not identified. Halite is somewhat more common and less coarse in Zag than in Monahans (see below).

The halite grains in Zag (Fig. 4) are well crystallized, but do not exhibit sharp cubic morphology as do those in Monahans; instead, many grains are fractured and have irregular shapes. The analysis of a representative Zag halite (Table 3) shows that K is less abundant than in Monahans halite; also unlike Monahans halite, there are no Br-rich areas.

Aqueous fluid inclusions are present in Zag halite. These inclusions have a maximum size of ~10 μm, although most are smaller than 5 μm. Inclusions have negative crystal shapes which tend to be approximately cubic as is the case for liquid fluid inclusions in unrecrystallized bedded salt deposits on Earth (Roedder, 1984). Both primary inclusions (incorporated into growing halite crystals) and secondary inclusions (trapped inside previously formed halite crystals when fluid-filled

TABLE 3. Results of individual electron microprobe analyses of halite and sylvite.

	Na	Cl	K	Br	Total	Na	Cl	K	Br
	(wt%)					(atom%)			
Monahans-1	35.4	59.5	0.91	0.23	96.0	47.5	51.7	0.71	0.089
Monahans-2	39.0	62.9	0.10	0.19	102.2	48.8	51.1	0.08	0.069
Monahans-3	5.5	49.9	43.8	0.44	99.6	8.6	50.8	40.5	0.200
Zag-1	38.1	62.6	0.06	0.35	101.1	48.3	51.6	0.00	0.128

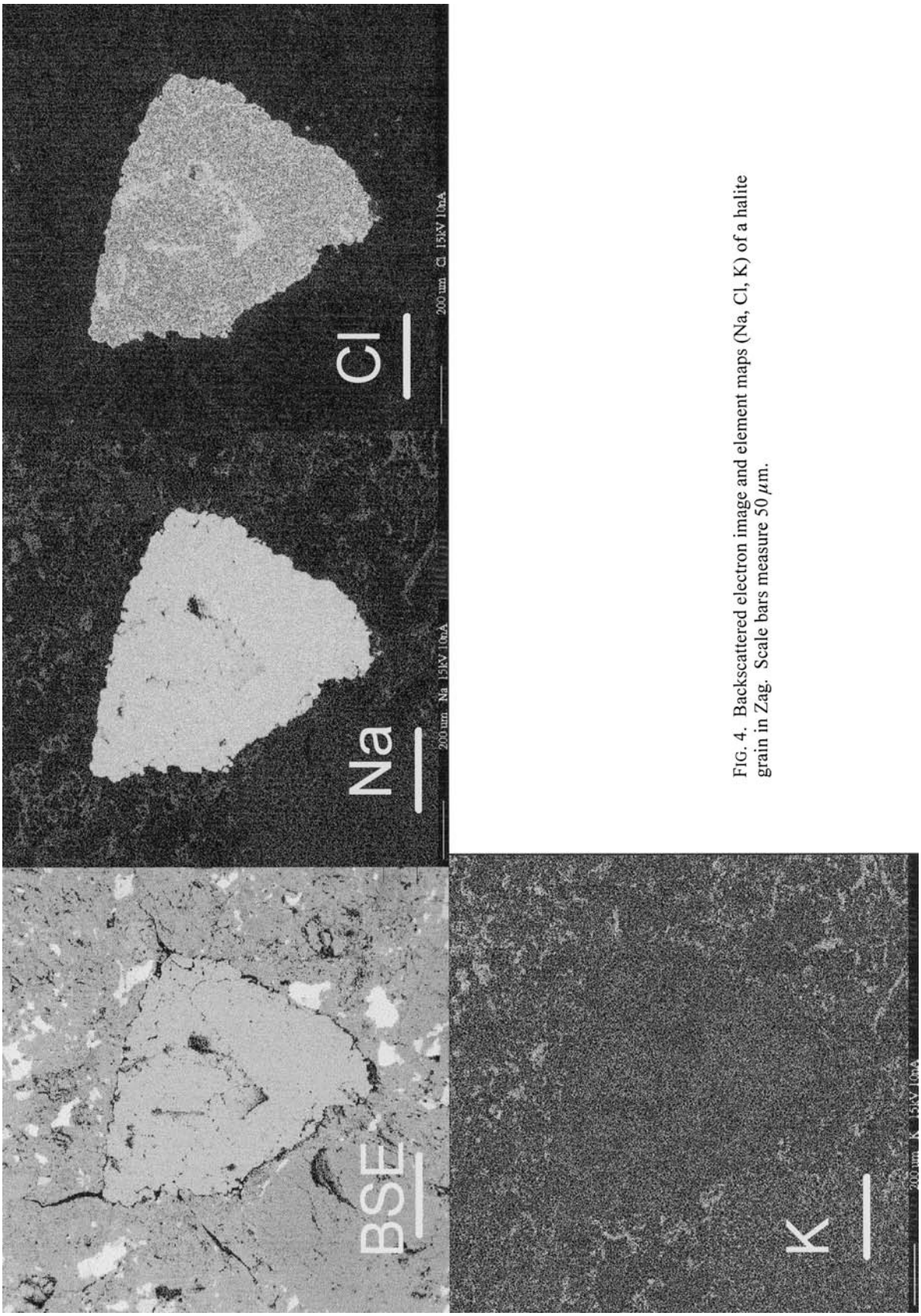

FIG. 4. Backscattered electron image and element maps (Na, Cl, K) of a halite grain in Zag. Scale bars measure 50 μm.

fractures heal) are present. The number of fluid inclusions in Zag halite is significantly higher than in Monahans halite. The paucity of vapor bubbles in the Zag inclusions suggests that the aqueous fluids were trapped at low temperatures (≤100 °C; probably 25–50 °C). They have not appreciably leaked since trapping. The small size of the fluid inclusions has precluded additional analyses.

Petrographic, Mineralogic and Geochemical Characteristics of Monahans

Whole-Rock–Monahans is a matrix-supported breccia consisting of light-colored metamorphic clasts and dark clasts exhibiting extensive silicate darkening set within a gray, clastic matrix exhibiting moderate silicate darkening (Fig. 5). In the small portions available to us, the light-colored clasts constitute ~65 vol%, dark clasts ~5%, and the clastic matrix ~30 vol%. However, these proportions may not be representative of the whole rock. Bogard *et al.* (2001) determined that the clastic matrix of Monahans (called "dark" by them) contains moderate concentrations of implanted solar gases, indicating that this material once resided in the parent-body regolith. The light-colored metamorphic clasts contain orders of magnitude lower concentrations of solar gases; the dark clasts (called "clasts" by Bogard *et al.*) are intermediate in their noble gas concentrations. All of the Monahans lithologies are H5, despite their quite different appearances.

Light-Colored Metamorphic Clasts–The light-colored clasts in the 1.2 kg Monahans stone range up to 1.5 cm in maximum dimension and have subrounded to subangular shapes. They exhibit moderately recrystallized textures consistent with petrologic type 5; the chondrules do not contain glass, and olivine and low-Ca pyroxene compositions are relatively equilibrated. Olivine ($Fa_{18.8\pm0.5}$; $n = 44$) and low-Ca pyroxene ($Fs_{18.5\pm0.5}$; $n = 40$) have the same compositions in all three clasts analyzed. Olivine is within the established range for H-group chondrites ($Fa_{17.3–20.2}$; Rubin, 1990), but low-Ca pyroxene has a mean composition slightly beyond the established range ($Fs_{15.7–18.1}$; Gomes and Keil, 1980). A representative analysis of low-Ca pyroxene is shown in Table 4. Olivine contains a maximum of 0.7 ± 0.2 wt% CaO. Small grains of diopside are also present. Only a few grains of

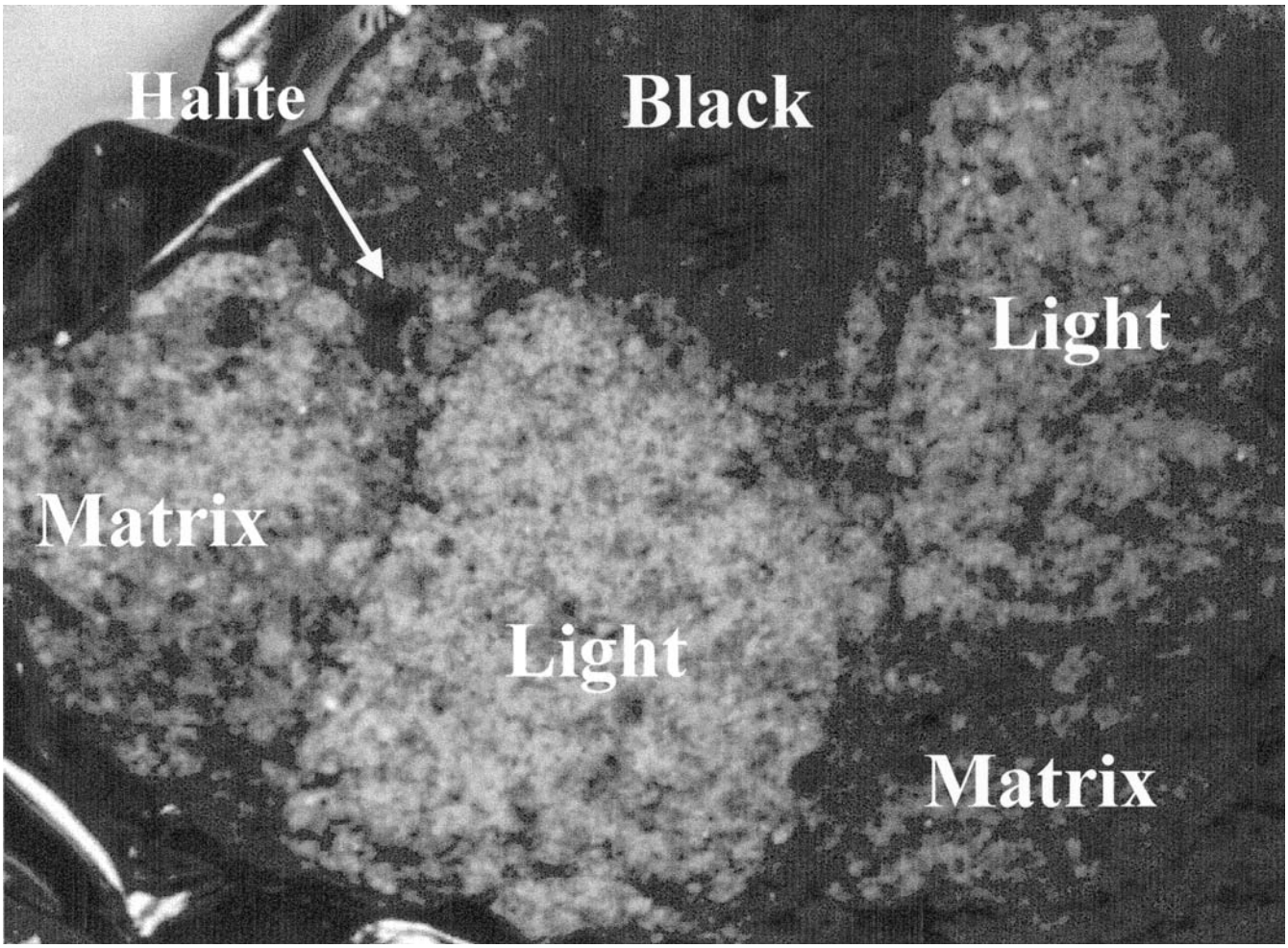

FIG. 5. The Monahans meteorite, showing the brecciated texture with light-colored metamorphic clasts, silicate-darkened black clasts, and the halite-containing gray matrix. Field of view is 3 cm. Reflected light.

TABLE 4. Representative analyses (wt%) of olivine and low-Ca pyroxene in Monahans (1998).

	Olivine	Low-Ca pyx
Clast type	dark	light
SiO_2	39.6	56.3
TiO_2	<0.04	0.14
Al_2O_3	<0.04	0.16
Cr_2O_3	<0.04	0.16
FeO	17.7	11.0
MgO	42.4	30.9
CaO	<0.04	0.77
Na_2O	<0.04	<0.04
K_2O	<0.04	<0.04
Total	99.7	99.4
Fa (mol%)	19.0	–
Fs (mol%)	–	16.4
Wo (mol%)	–	1.5

plagioclase were analyzed ($Ab_{72\pm2.2}Or_{18\pm1.1}$; n = 4); these are appreciably potassic, as are a minority of grains in other OC regolith breccias (Fig. 6 of Bischoff *et al.*, 1983). Kamacite contains 6.5 ± 0.7 wt% Ni. Martensite averaging ~16 wt% Ni also occurs. Troilite is essentially pure FeS.

Olivine within the light-colored clasts exhibits undulatory extinction and irregular fractures, indicative of shock stage S2.

Dark Clasts Exhibiting Silicate Darkening–The dark clasts range up to 1 cm in maximum dimension and tend to have rounded, elongated shapes. They have recrystallized textures and relatively equilibrated olivine and low-Ca pyroxene compositions consistent with petrologic type 5; chondrules contain no apparent glass.

We analyzed only one dark clast and obtained the following mean compositions: olivine ($Fa_{19.0\pm0.5}$; n = 32) and low-Ca pyroxene ($Fs_{18.2\pm0.5}$; n = 62). A representative analysis of olivine is shown in Table 4. Olivine contains a maximum of 0.7 ± 0.2 wt% CaO (identical to those in the light-colored clasts). No diopside was identified. A few grains of moderately potassic plagioclase were also analyzed ($Ab_{74\pm1.9}Or_{8\pm1.3}$; n = 3). Kamacite averages 6.9 ± 0.7 wt% Ni. Martensite averaging ~14 wt% Ni is also present. Troilite is essentially pure FeS.

Shock effects within the dark clasts are much more pronounced than in the light-colored clasts. Olivine grains exhibit undulatory extinction, irregular fractures, planar fractures and weak-to-moderate mosaicism, characteristic of shock stage S4. The extensive silicate darkening in these clasts is caused by abundant melt pockets, veins of metallic Fe-Ni and troilite, and curvilinear trails of tiny metal and troilite blebs.

Matrix Regions–Matrix regions are ubiquitous on broken surfaces of Monahans. They possess a fractured and recrystallized texture and contain relatively equilibrated olivine and low-Ca pyroxene. Chondrules contain no apparent glass. Halite and sylvite (see below) are confined exclusively to the matrix.

Olivine (19.0 ± 0.5; n = 22) and low-Ca pyroxene ($Fs_{18.0\pm0.4}$; n = 26) are within the ranges established for H-group chondrites. Olivine contains a maximum of 0.6 ± 0.2 wt% CaO. No diopside grains were identified. Kamacite contains 6.9 ± 0.7 wt% Ni. A few grains of martensite containing ~14 wt% Ni also occur. Troilite is essentially pure FeS.

Shock effects within the matrix are intermediate between those in the light and dark clasts. Olivine exhibits undulatory extinction, irregular fractures and planar fractures, characteristic of shock stage S3. Only a few olivine grains display weak mosaic extinction.

Halite Grains–The gray matrix of Monahans contains scattered dark blue to purple, transparent to opaque, halite grains (ranging up to 5 mm in size) with minor inclusions of sylvite. The discovery of halite and sylvite in Monahans marked the first occurrence of these minerals in ordinary chondrites (Zolensky *et al.*, 1999a). (Halite and sylvite were reported previously in ureilites (Berkeley *et al.*, 1979) and in a hydrocarbon mass in CM2 Murchison (Barber, 1981).) The individual halite grains in Monahans appear to be the coarsest examples of these minerals known from any meteorite.

The halite grains are well crystallized, and exhibit sharp cubic morphology. The sharp crystal faces of at least some of the halite grains occur within small voids. Crystals of sylvite are distributed heterogeneously as inclusions within the larger halite crystals, similar to the occurrence of halite and sylvite in terrestrial rocks. Halite contains minor K and Br; sylvite contains significant Na and minor Br (Table 3). X-ray element maps show that Br concentrations are slightly higher in sylvite than halite (Fig. 6).

Aqueous fluid inclusions in Monahans halite were described by Zolensky *et al.* (1999a). These inclusions have a maximum size of ~15 μm, although most are smaller than 10 μm. Both primary (Fig. 7) and secondary (Fig. 8) inclusions are present. The paucity of vapor bubbles in the inclusions suggests that they were trapped at low temperatures (≤100 °C), and did not suffer significant post-trapping leakage. The inclusion fluid-freezing temperatures indicate that the inclusions contain divalent cations such as Fe, Mg and/or Ca (Zolensky *et al.*, 1999a).

DISCUSSION

Preterrestrial Origin of the Halite

Halite is an abundant mineral on Earth, occurring in marine evaporite deposits, atolls, coastal lagoons, coastal intertidal and supratidal zones, playa deposits in enclosed basins, salt domes, and some igneous rocks. It is thus important to determine if the halite in Zag and Monahans could be terrestrial contaminants. There are four arguments for the preterrestrial origin of halite in these meteorites.

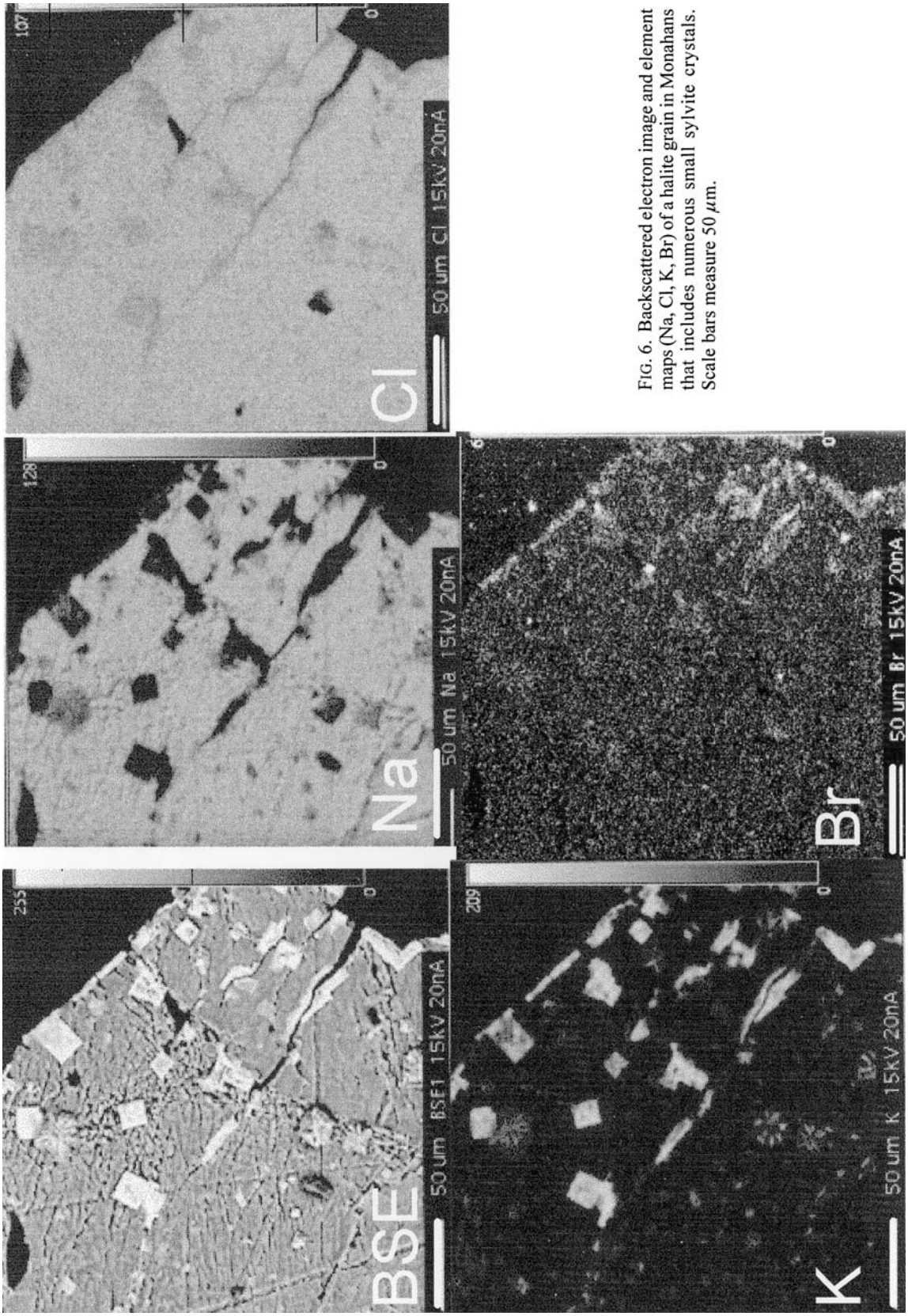

FIG. 6. Backscattered electron image and element maps (Na, Cl, K, Br) of a halite grain in Monahans that includes numerous small sylvite crystals. Scale bars measure 50 μm.

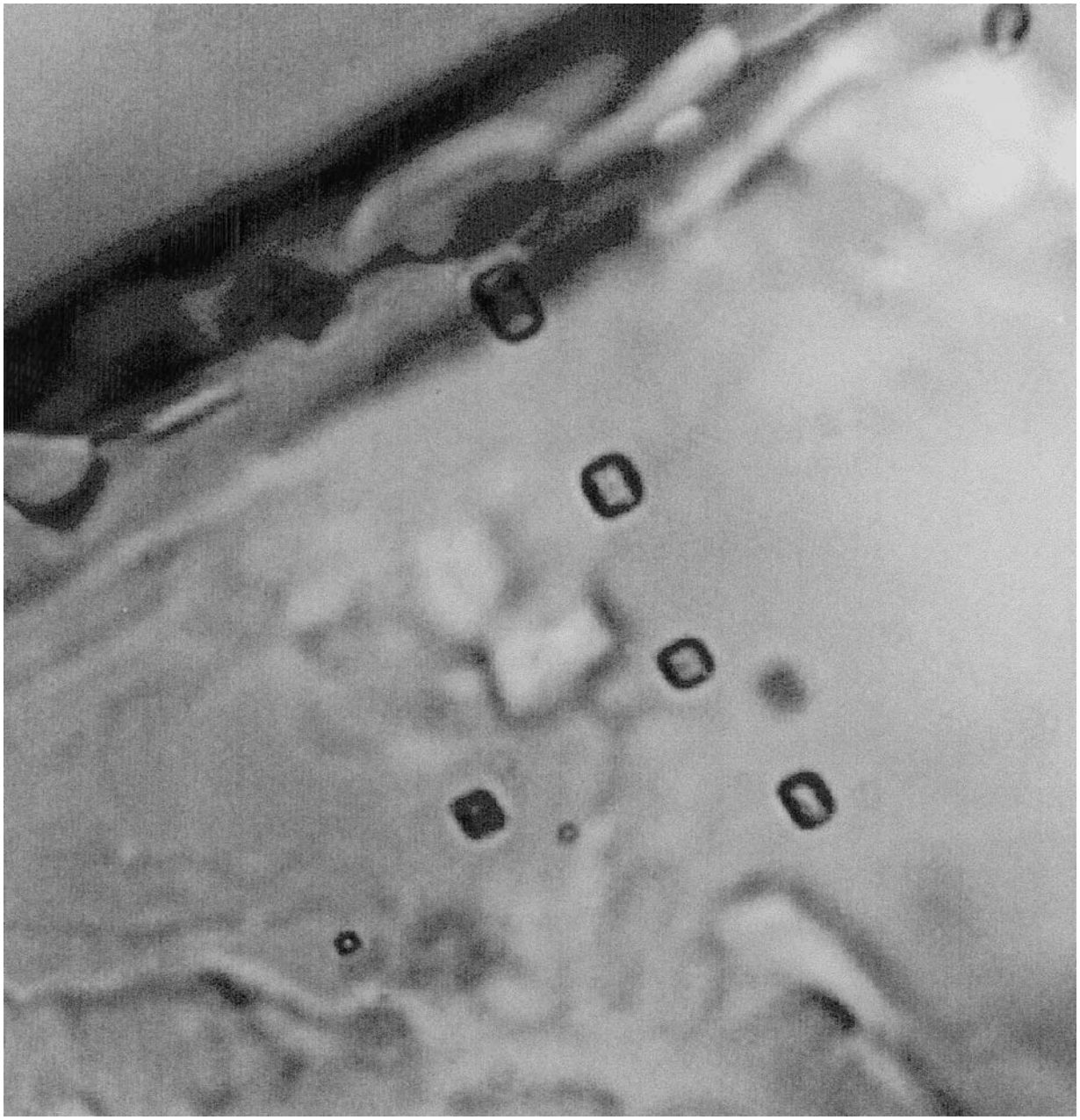

FIG. 7. Primary aqueous fluid inclusions (dark-lined rectangles) within a Monahans halite crystal. Field of view is 50 μm. Transmitted light.

(1) Zag and Monahans are fresh falls. Eyewitness accounts of the Monahans fall indicate that one of the two Monahans stones was picked up very soon after landing (within 1 min) by neighborhood boys who reported that the stone was still warm. There was thus little opportunity for salt contamination. The second Monahans stone was collected the following day. The town of Monahans is located in a desert region of Texas, and there had been no precipitation between the time of the meteorite fall and the collection of the stones. The stones were placed in police evidence bags soon after recovery, and never washed. The stones were opened in the NASA Johnson Space Center's Meteorite Processing Laboratory within 3 days of recovery using a chisel and hammer; no samples were sawed.

(2) Halite is widely distributed in the matrix regions of both Zag and Monahans. It is very unlikely that terrestrial briny fluids could have penetrated these different regions during the short period of time that these stones were on the ground. Ordinary chondrite porosities and permeabilities are very small (Corrigan *et al.*, 1997), and it is not possible that terrestrial

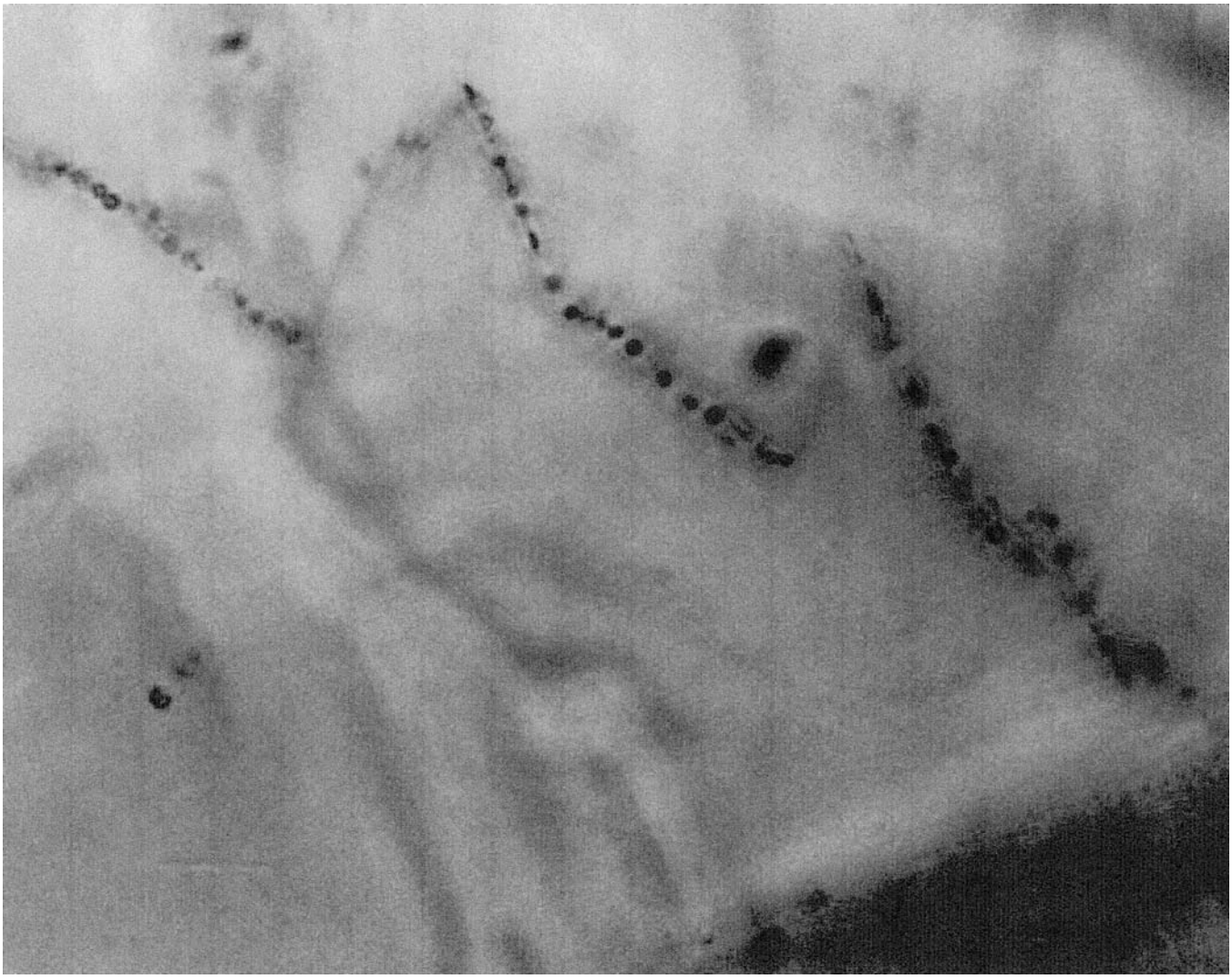

FIG. 8. Secondary aqueous fluid inclusions (small dark rectangles) aligned along healed fractures within a Monahans halite crystal. Field of view is 50 μm. Transmitted light.

halite crystals touching the surface of the stones could have penetrated the interiors of the meteorites.

(3) Exposure of halite to ionizing radiation produces the same blue-to-purple color observed in Monahans and Zag halite (Nassau, 1983), although this can also be caused by the presence of colloidal inclusions (Deer *et al.*, 1962). We suggest that the halite coloration was produced in Zag and Monahans either by exposure to solar and galactic cosmic rays or by exposure to beta decaying ^{40}K (in the sylvite). The coloring mechanism is electron trapping in Cl^- vacancies. We have not performed the simple heating experiments to verify the electron color center mechanism in the meteoritic halite for fear of compromising the fluid inclusions; nevertheless, it is expected that the halite would lose coloration between 100 and 500 °C (K. Nassau, pers. comm., 1999). Although there are several well-known terrestrial deposits of blue rock salt (*e.g.*, Kirchheimer, 1976), halite in the vast majority of terrestrial evaporite deposits is white or clear. Therefore, the blue color of the Zag and Monahans halite strongly supports (but does not prove) a preterrestrial origin.

(4) The Ar-Ar ages of the halite grains show them to be older than extant terrestrial rocks. Since halite generally contains impurities of unstable isotopes of I, K, Rb, and their daughter products, many chronologic systems are applicable. L. Nyquist (JSC) and co-workers determined a Rb-Sr model age of Monahans halite to be 4.7 ± 0.2 Ga, which Zolensky *et al.* (1999a) concluded was the formation age. Whitby *et al.* (2000) used I/Xe to determine ages of 4.03 ± 0.005 and 4.66 ± 0.08 Ga for two Zag halite grains. Bogard *et al.* (2001) used $^{39}Ar/^{40}Ar$ to determine a minimum formation age of Monahans halite grains to be 4.33 ± 0.01 Ga. These ages unambiguously demonstrate an ancient age and therefore a preterrestrial origin of Zag and Monahans halite.

Petrogenetic History of Components in Zag and Monahans

Light-Colored Clasts–The H5 and H6 clasts in Zag and the H5 clasts in Monahans formed from less-equilibrated, less-recrystallized, H3-like material by thermal metamorphism. Some material in Zag was metamorphosed to a greater extent than other material. During heating, chondrule glass devitrified, matrix grains coarsened, chondrules and matrix became texturally more integrated, plagioclase, Ca-pyroxene and chromite grew, and mineral compositions equilibrated.

After metamorphism, the H5 and H6 rocks in Zag were shocked to different extents, broken into fragments and deposited into the regolith. The H5 clasts in Monahans experienced a similar history. During the shock events, some metallic Fe-Ni, troilite and chromite were melted and injected into fractures, producing silicate darkening (Rubin, 1992) and shock veins (*e.g.*, Stöffler *et al.*, 1991). Some chromite-plagioclase associations were melted and recrystallized. Some shock-melted metal-troilite assemblages precipitated metallic Cu during cooling (Rubin, 1994).

Dark Clasts–It is evident that the dark clasts formed from light-colored metamorphosed H-chondrite material. Light clasts and dark clasts in Zag are metamorphosed (H4–H6) and have indistinguishable mineral compositions. The single analyzed dark clast in Monahans is an H5 chondrite, as are the light-colored clasts. The dark clasts in these meteorites formed from metamorphosed H-chondrite material that was shocked and developed extensive silicate darkening. Significant amounts of the metallic Fe-Ni and troilite were melted and injected into and around silicate grains. Some melted troilite filled fractures in unmelted chromite grains. An appreciable fraction of the chromite within Zag dark clasts was shock melted and injected into fractures as veinlets and aligned blebs. Many olivine grains developed mosaic extinction. Some coarse metal and troilite grains were melted and quenched, forming fine-grained cellular and dendritic assemblages. Metallic Cu in the Zag dark clasts precipitated in some melted metal-troilite assemblages. Some melted metal mixed with melted silicate grains and formed apparently sheared metal-silicate assemblages.

Impact-Melt-Rock Clasts–Chondrule-free Zag clast A3 probably formed by impact melting of H-chondrite material. Chondrules were melted and shattered, although a few chondrule fragments survived. Metal and sulfide melted; some assemblages incorporated shattered silicate grains. Fine-grained silicates precipitated from the melt; because the shock pressure had already been released, these small silicate grains were not strained.

Although the melt-rock clast in Zag matrix region D1 probably formed from normal H-chondrite material, it is unusually rich in metal and troilite (~65 wt%). Because silicate and metal-troilite form immiscible melts during impact-melting events (*e.g.*, Wilkening, 1978), it is possible that this clast is a fragment of the partially separated metal-troilite-rich portion of the melt.

Matrix Regions and Halite Deposition–In both Zag and Monahans, impact gardening shattered light-colored metamorphic rocks, silicate-darkened rocks and impact-melt rocks. Fragments of these materials were dumped into the regolith. Micrometeoroid impacts into the regolith caused additional pulverization and silicate darkening (as metal and troilite were melted and mobilized). This regolithic material became the matrices of the meteorites. We hypothesize that the halite in these meteorites originated on the H-chondrite parent asteroid. Because of the fine grain size of the porous regolith, aqueous fluids were able to flow through it. By analogy with the compositional characteristics of the porous outer zones of bleached chondrules (Grossman *et al.*, 2000), it seems likely that the aqueous fluids preferentially dissolved alkalies, Al, and perhaps Ca, possibly from chondrule mesostases. Dissolution of mafic silicates may have contributed Mg and Fe; dissolution of fine-grained chlorapatite grains may have contributed Cl to the aqueous fluids.

Evaporation of water from the brines near the parent-body surface increased the halite and sylvite concentrations in the residual liquid. When the brines became supersaturated, grains of halite precipitated.

Rapid precipitation of halite causes large numbers of fluid inclusions to be trapped in terrestrial environments (Roedder, 1984); because the abundance of fluid inclusions in the Zag and Monahans halite is low, it seems likely that the halite in these meteorites precipitated fairly slowly. This is supported by the euhedral shapes of the halite grains and the lack of chevron textures (*i.e.*, upward-pointing growth zones that form when crystal edges grow faster than face centers).

Nearby micrometeorite impacts probably caused many of the halite grains to fracture, particularly those in Zag. Healing of fluid-filled fractures trapped secondary fluid inclusions.

The somewhat irregular boundaries between some halite grains and the enclosing matrix suggest that halite precipitated *in situ* on the irregular surface and grew out into a void. Similarly, the occurrence of small voids surrounding the sharp crystal faces of many halite grains in Monahans suggests that the halite grains grew into available voids.

Source of Water

The source of the water responsible for aqueous alteration on OC parent bodies must have been either melted ice or dehydrated phyllosilicates. Accreted ice seems unlikely because nebular temperatures were probably not low enough in the vicinity of the asteroid belt (~3 AU) during the time the nebula was still present for ice to condense. Nebular models (*e.g.*, Cameron, 1995) place the "snow line" at about Jupiter's 5.2 AU distance from the Sun.

Exogenous ice delivered by impacting icy planetesimals cannot be ruled out, but given the widespread distribution of aqueous alteration effects (*e.g.*, bleached chondrules) in all three

OC groups (Grossman *et al.*, 2000), it seems unlikely that such collisions could be the main source of water.

Phyllosilicate formation by solid-solid diffusion is inhibited in the solar nebula, requiring times longer than the age of the solar system (Fegley and Prinn, 1989). However, Petaev and Wood (1998) calculated that some phyllosilicates could condense from a gas of solar composition at temperatures of about 330–400 K if small amounts (0–0.2%) of the condensate are removed continuously from the gas.

It also seems plausible that, during chondrule formation, Al, Fe, Mg, Si, O, Na and K were commonly evaporated from some chondrule precursor materials. J. T. Wasson (pers. comm., 2001) speculated that when local H_2O-bearing gas became enriched in these elements, condensation of phyllosilicates might have occurred. Phyllosilicates would have subsequently agglomerated with chondrules, metal and sulfide grains, fine-grained matrix material, and other components to form chondritic asteroids.

Serpentine and saponite begin to dehydrate at ~500 °C (*e.g.*, Lipschutz *et al.*, 1999). Such temperatures could have been reached in the interiors of chondritic parent bodies by the decay of the long-lived radionuclides ^{40}K, ^{232}Th, ^{235}U and ^{238}U. Released water could have migrated toward the surface of the asteroid causing aqueous alteration enroute. However, it is unlikely that temperatures ≥500 °C could have been reached in asteroidal interiors within the few million years allowed by the formation ages of the halite grains in Zag (which are only ~2 Ma younger than the oldest known solar-system minerals; Whitby *et al.*, 2000).

Alternatively, phyllosilicate dehydration could have been caused by numerous low-energy impact events. The likelihood of such events is indicated by the observation that most OC appear to be fragmental breccias (Scott *et al.*, 1985; Rubin, 1990; Rubin and Brearley, 1996). The impacts that caused the widespread brecciation of OC could have provided the heat necessary in localized regions to dehydrate phyllosilicates. It seems possible that some halite grains on the parent body could have formed much later, after late-stage impacts dehydrated phyllosilicates and caused mobilization of aqueous fluids.

Summary of Parent-Body Processes

Zag and Monahans experienced a complex set of parent-body modification processes. After agglomeration, the H-chondrite parent body consisted of unequilibrated primitive nebular materials—predominantly chondrules, chondrule fragments, metal and sulfide grains, and fine-grained silicate matrix material containing rare phyllosilicate grains. Heating to 600–950 °C (Dodd, 1981) was caused either by planetesimal collisions (*e.g.*, Wasson *et al.*, 1987; Cameron *et al.*, 1990; Rubin, 1995) or the decay of ^{26}Al (*e.g.*, Reeves and Audouze, 1968; Grimm and McSween, 1993). By the end of this process, large blocks of light-colored metamorphosed H chondrites were produced.

Subsequent to thermal metamorphism, the rocks were shocked. Significant fractions of the metallic Fe-Ni and troilite were melted and mobilized, leading to silicate darkening of the light-colored clasts (Rubin, 1992). In those rocks where silicate darkening was extensive, dark clasts were produced (*e.g.*, Williams *et al.*, 1985). In some of the locations where chromite and plagioclase were juxtaposed, these phases melted and chromite-plagioclase associations formed (*e.g.*, Rubin *et al.*, 2001). In a few regions, metal-troilite assemblages were melted and quenched, producing fine-grained cellular and dendritic metal-troilite intergrowths (Scott, 1982). Metallic Cu became supersaturated in the residual sulfide-rich liquid of some melted metal-troilite assemblages. It eventually precipitated at available sites with high surface energies, generally at metal-troilite grain boundaries (Rubin, 1994).

Impact gardening fragmented the metamorphosed H-chondrite blocks. Micrometeorite impacts pulverized the fragments and produced a clastic regolith. Continuing impact events deposited additional H4, H5 and H6 chips into the regolith. Hypervelocity impacts into the regolith and into the light-colored metamorphosed fragments created small blobs of chondritic melt that crystallized into impact-melt rocks (*e.g.*, Fodor and Keil, 1975, 1976; Wilkening, 1978). These also became incorporated into the regolith.

Solar-wind noble gases bombarded the regolith and gas molecules were adsorbed onto regolithic mineral grains (*e.g.*, Suess *et al.*, 1964). The non-porous nature of the light-colored and dark clasts precluded significant adsorption of solar-wind particles.

The old ages of the Zag and Monahans halite grains (Zolensky *et al.*, 1999a; Whitby *et al.*, 2000; Bogard *et al.*, 2001) indicate that aqueous alteration occurred very early in solar-system history, probably within a few million years of accretion. Because the inferred duration of thermal metamorphism was far longer than this (Göpel *et al.*, 1994), aqueous alteration and halite precipitation must have occurred on the parent body during the epoch of metamorphism. However, because the fluid inclusions within the halite grains were trapped at low temperatures (≤100 °C) (Zolensky *et al.*, 1999a), halite precipitation must have occurred in portions of the parent body that were not significantly heated.

The aqueous fluids, which formed from dehydrated phyllosilicates, percolated through cold regolithic regions of the asteroid. The fluids contained alkalies, Cl and small concentrations of divalent cations (*i.e.*, Fe^{2+}, Mg^{2+}, Ca^{2+}), probably acquired during low-level leaching of minerals and chondrule glass in the regolith. The local regolithic regions gradually lost water vapor (probably to space) causing the residual brines to become supersaturated in halides; halite and halite-sylvite intergrowths precipitated in the porous regolith and trapped fluid inclusions. Ar-Ar release patterns for the Zag whole rock show plateaus that have a mean inferred age of 4.25 ± 0.03 Ga (Whitby *et al.*, 2000), suggesting that Zag brecciation occurred at this time. Such impacts may also have

been responsible for the disturbance of the I-Xe systematics of the Zag halite noted by Whitby *et al.* (2000).

The critical factor controlling the deposition of halite on an asteroid was probably the availability of soluble Cl in the bulk rock. Total Cl in chondritic meteorites ranges from 10 to 300 μg/g, and the water soluble fraction of this Cl can be as low as 10% (Tarter, 1981; Garrison *et al.*, 2000). Using these measured values, it is possible to estimate roughly the minimum amount of chondritic rock necessary to provide the quantity of halides observed in Monahans and Zag. A mass of 2 to 600 kg of chondritic rock must have been totally leached of water-soluble Cl to yield the observed halide grains. Because leaching at low temperatures is inefficient, a much greater quantity of rock is required. Even more mass is required if the rock is not significantly porous and permeable. Great quantities of rock require large amounts of water.

During crystallization, the salt grains trapped droplets of fluid, forming primary fluid inclusions. Low-energy impacts fractured some of the brittle halite grains allowing the brine to penetrate. Healing of fluid-filled fractures produced secondary fluid inclusions.

Late-stage impact events into the regolith caused minor melting along grain boundaries, a presumptive decrease in the concentrations of solar-wind gases, and lithification of the Zag and Monahans breccias. This process may have been repeated several times. Eventually, impact events launched Zag and Monahans off of the H-chondrite parent body. In the case of Monahans, this event occurred 6.0 ± 0.5 Ma ago (Bogard *et al.*, 2001).

Acknowledgments–We are grateful to Edwin Thompson for providing most of the Zag materials used in this study and for first identifying the halite. We thank E. Gibson for obtaining the Monahans sample. We also thank the townspeople of Monahans, Texas for the loan of their meteorite. We appreciate J. T. Wasson's helpful comments and are grateful to V. Yang and L. Le for critical assistance with the microprobe halide analyses at J.S.C. We thank J. N. Grossman and M. K. Weisberg for their helpful reviews. This work was supported in part by NASA grants NAG5-4766 (A. E. Rubin), 344-36-99-02 (M. E. Zolensky), and NAG5-10733 (R. J. Bodnar).

Editorial handling: C. M. Pieters

REFERENCES

BARBER D. (1981) Matrix phyllosilicates and associated minerals in C2M carbonaceous chondrites. *Geochim. Cosmochim. Acta* **45**, 945–970.

BERKELEY J., TAYLOR G. J. AND KEIL K. (1979) Fluorescent accessory phases in the carbonaceous matrix of ureilites. *Geophys. Res. Lett.* **5**, 1075–1078.

BISCHOFF A., RUBIN A. E., KEIL K. AND STÖFFLER D. (1983) Lithification of gas-rich chondrite regolith breccias by grain boundary and localized shock melting. *Earth Planet. Sci. Lett.* **66**, 1–10.

BOGARD D. D., GARRISON D. H. AND MASARIK J. (2001) The Monahans chondrite and halite: Argon-39/argon-40 age, solar gases, cosmic-ray exposure ages, and parent body regolith neutron flux and thickness. *Meteorit. Planet. Sci.* **36**, 107–122.

BRIDGES J. C. AND GRADY M. M. (2000) Petrography and fluid inclusion studies of Zag (abstract). *Meteorit. Planet. Sci.* **35 (Suppl.)**, A33–A34.

CAMERON A. G. W. (1995) The first ten million years in the solar nebula. *Meteoritics* **30**, 133–161.

CAMERON A. G. W., BENZ W. AND WASSON J. T. (1990) Heating during asteroidal collisions (abstract). *Lunar Planet. Sci.* **21**, 155–156.

CHOI B-G., MCKEEGAN K. D., KROT A. N. AND WASSON J. T. (1998) Extreme oxygen-isotope compositions in magnetite from unequilibrated ordinary chondrites. *Nature* **392**, 577–579.

CORRIGAN C. C., ZOLENSKY M. E., DAHL J., LONG M., WEIR J. AND SAPP C. (1997) The porosity and permeability of chondritic meteorites and interplanetary dust particles. *Meteorit. Planet. Sci.* **32**, 509–515.

DEER W. A., HOWIE R. A. AND ZUSSMAN J. (1962) *Rock-Forming Minerals, Vol. 5, Nonsilicates*. Longmans Pub. Co., London, U.K. 371 pp.

DODD R. T. (1969) Metamorphism of the ordinary chondrites: A review. *Geochim. Cosmochim. Acta* **33**, 161–203.

DODD R. T. (1981) *Meteorites—A Petrologic–Chemical Synthesis*. Cambridge Univ. Press, Cambridge, U.K. 368 pp.

DODD R. T. AND JAROSEWICH E. (1979) Incipient melting and shock classification of L-group chondrites. *Earth Planet. Sci. Lett.* **44**, 335–340.

FEGLEY B. AND PRINN R. G. (1989) Solar nebula chemistry: Implications for volatiles in the solar system. In *The Formation and Evolution of Planetary Systems* (eds. H. A. Weaver and L. Danly), pp. 171–211. Cambridge Univ. Press, Cambridge, U.K.

FODOR R. V. AND KEIL K. (1975) Implications of poikilitic textures in LL-group chondrites. *Meteoritics* **10**, 325–339.

FODOR R. V. AND KEIL K. (1976) Carbonaceous and noncarbonaceous lithic fragments in the Plainview, Texas chondrite: Origin and history. *Geochim. Cosmochim. Acta* **40**, 177–189.

FREDRIKSSON K. AND KEIL K. (1963) The light-dark structure in the Pantar and Kapoeta stone meteorites. *Geochim. Cosmochim. Acta* **27**, 717–739.

GARRISON D., HAMLIN S. AND BOGARD D. (2000) Chlorine abundances in meteorites. *Meteorit. Planet. Sci.* **35**, 419–429.

GOMES C. B. AND KEIL K. (1980) *Brazilian Stone Meteorites*. Univ. New Mexico Press, Albuquerque, New Mexico, USA. 162 pp.

GÖPEL C., MANHES G. AND ALLÈGRE C. J. (1994) U-Pb systematics of phosphates from equilibrated ordinary chondrites. *Earth Planet. Sci. Lett.* **121**, 153–171.

GRADY M. M. (2000) *Catalogue of Meteorites*. Fifth edition. Cambridge Univ. Press, Cambridge, U.K. 689 pp.

GRIMM R. E. AND MCSWEEN H. Y. (1993) Heliocentric zoning of the asteroid belt by aluminum-26 heating. *Science* **259**, 653–655.

GROSSMAN J. N., ALEXANDER C. M. O'D. AND BREARLEY A. J. (2000) Bleached chondrules: Evidence for widespread aqueous processes on the parent asteroids of ordinary chondrites. *Meteorit. Planet. Sci.* **35**, 467–486.

HUTCHISON R., ALEXANDER C. M. O'D. AND BARBER D. J. (1987) The Semarkona meteorite; First recorded occurrence of smectite in an ordinary chondrite, and its implication. *Geochim. Cosmochim. Acta* **51**, 1875–1882.

KIRCHHEIMER F. (1976) Über Steinsalz und sein Vorkommen im Neckar- und Oberrheingebiet. *Bundesant. Geowiss., Geol. Jahrb. [D]* **18**, 1–139.

KÖNIG H., KEIL K., HINTENBERGER H., WLOTZKA F. AND BEGEMANN F. (1961) Untersuchungen an Steinmeteoriten mit extrem hohem Edelgasgehalt. I, Der Chondrit Pantar. *Zeitschrift für Naturforschung* **16a**, 1124–1130.

KROT A. N., ZOLENSKY M. E., WASSON J. T., SCOTT E. R. D., KEIL K. AND OHSUMI K. (1997) Carbide-magnetite

assemblages in type-3 ordinary chondrites. *Geochim. Cosmochim. Acta* **61**, 219–237.

LIPSCHUTZ M. E. AND WOOLUM D. S. (1988) Highly labile elements. In *Meteorites and the Early Solar System* (eds. J. F. Kerridge and M. S. Matthews), pp. 462–487. Univ. Arizona Press, Tucson, Arizona, USA.

LIPSCHUTZ M. E., ZOLENSKY M. E. AND BELL M. S. (1999) New petrographic and trace element data on thermally metamorphosed carbonaceous chondrites. *Proc. NIPR Symp. Antarct. Meteorites* **12**, 57–80.

MCSWEEN H. Y., SEARS D. W. G. AND DODD R. T. (1988) Thermal metamorphism. In *Meteorites and the Early Solar System* (eds. J. F. Kerridge and M. S. Mathews), pp. 102–113. Univ. Arizona Press, Tucson, Arizona, USA.

NASSAU K. (1983) *The Physics and Chemistry of Color*. John Wiley & Sons, New York, New York, USA. 454 pp.

PETAEV M. I. AND WOOD J. A. (1998) The condensation with partial isolation (CWPI) model of condensation in the solar nebula. *Meteorit. Planet. Sci.* **33**, 1123–1137.

POWERS M. C. (1953) A new roundness scale for sedimentary particles. *J. Sed. Pet.* **23**, 117–119.

REEVES H. AND AUDOUZE J. (1968) Early heat generation in meteorites. *Earth Planet. Sci. Lett.* **4**, 135–141.

ROEDDER E. (1984) *Fluid Inclusions*. Rev. Mineral. **12**, Mineral. Soc. America, Washington, D.C., USA. 644 pp.

RUBIN A. E. (1990) Kamacite and olivine in ordinary chondrites: Intergroup and intragroup relationships. *Geochim. Cosmochim. Acta* **54**, 1217–1232.

RUBIN A. E. (1992) A shock-metamorphic model for silicate darkening and compositionally variable plagioclase in CK and ordinary chondrites. *Geochim. Cosmochim. Acta* **56**, 1705–1714.

RUBIN A. E. (1994) Metallic copper in ordinary chondrites. *Meteoritics* **29**, 93–98.

RUBIN A. E. (1995) Petrologic evidence for collisional heating of chondritic asteroids. *Icarus* **113**, 156–167.

RUBIN A. E. AND BREARLEY A. J. (1996) A critical evaluation of the evidence for hot accretion. *Icarus* **124**, 86–96.

RUBIN A. E., SCOTT E. R. D., TAYLOR G. J., KEIL K., ALLEN J. S. B., MAYEDA T. K., CLAYTON R. N. AND BOGARD D. D. (1983) Nature of the H chondrite parent body regolith: Evidence from the Dimmitt breccia. *Proc. Lunar Planet. Sci. Conf.* **13th**, A741–A754.

RUBIN A. E., ULFF-MØLLER F., WASSON J. T. AND CARLSON W. D. (2001) The Portales Valley meteorite breccia: Evidence for impact-induced melting and metamorphism of an ordinary chondrite. *Geochim. Cosmochim. Acta* **65**, 323–342.

SCHULTZ L. AND FRANKE L. (2000) *Helium, Neon, and Argon in Meteorites—A Data Collection.* Max-Planck-Institut für Chemie, Mainz, Germany (CD-ROM).

SCHULTZ L. AND SIGNER P. (1977) Noble gases in the St. Mesmin chondrite: Implications to the irradiation history of a brecciated meteorite. *Earth Planet. Sci. Lett.* **36**, 363–371.

SCOTT E. R. D. (1982) Origin of rapidly solidified metal–troilite grains in chondrites and iron meteorites. *Geochim. Cosmochim. Acta* **46**, 813–823.

SCOTT E. R. D., LUSBY D. AND KEIL K. (1985) Ubiquitous brecciation after metamorphism in equilibrated ordinary chondrites. *Proc. Lunar Planet. Sci. Conf.* **16th**, D137–D148.

STÖFFLER D., KEIL K. AND SCOTT E. R. D. (1991) Shock metamorphism of ordinary chondrites. *Geochim. Cosmochim. Acta* **55**, 3845–3867.

SUESS H. E., WÄNKE H. AND WLOTZKA F. (1964) On the origin of gas-rich meteorites. *Geochim. Cosmochim. Acta* **28**, 595–607.

TANDON S. N. AND WASSON J. T. (1968) Gallium, germanium, indium and iridium variations in a suite of L-group chondrites. *Geochim. Cosmochim. Acta* **32**, 1087–1110.

TARTER J. G. (1981) The Abundance and Distribution of Chlorine in Meteorites. Ph.D. thesis, Arizona State University, Tempe, Arizona, USA. 170 pp.

VAN SCHMUS W. R. AND KOFFMAN D. M. (1967) Equilibration temperatures of iron and magnesium in chondritic meteorites. *Science* **155**, 1009–1011.

VAN SCHMUS W. R. AND RIBBE P. H. (1968) The composition and structural state of feldspar from chondritic meteorites. *Geochim. Cosmochim. Acta* **32**, 1327–1342.

VAN SCHMUS W. R. AND WOOD J. A. (1967) A chemical–petrologic classification for the chondritic meteorites. *Geochim. Cosmochim. Acta* **31**, 747–765.

WASSON J. T., BENZ W. AND RUBIN A. E. (1987) Heating of primitive, asteroid-size bodies by large impacts (abstract). *Meteoritics* **22**, 525–526.

WHITBY J., BURGESS R., TURNER G., GILMOUR J. AND BRIDGES J. (2000) Extinct ^{129}I in halite from a primitive meteorite: Evidence for evaporite formation in the early solar system. *Science* **288**, 1819–1821.

WILKENING L. L. (1978) Tysnes Island: An unusual clast composed of solidified, immiscible, Fe-FeS and silicate melt. *Meteoritics* **13**, 1–9.

WILLIAMS C. V., RUBIN A. E., KEIL K. AND SAN MIGUEL A. (1985) Petrology of the Cangas de Onis and Nulles regolith breccias: Implications for parent body history. *Meteoritics* **20**, 331–345.

WOOD J. A. (1962) Metamorphism in chondrites. *Geochim. Cosmochim. Acta* **26**, 739–749.

ZOLENSKY M. E., BODNAR R. J., GIBSON E. K., NYQUIST L. E., REESE Y., SHIH C-Y. AND WIESMANN H. (1999a) Asteroidal water within fluid inclusion-bearing halite in an H5 chondrite, Monahans. *Science* **285**, 1377–1379.

ZOLENSKY M. E., BODNAR R. J. AND RUBIN A. E. (1999b) Asteroidal water within fluid-inclusion-bearing halite in ordinary chondrites (abstract). *Meteorit. Planet. Sci.* **34 (Suppl.)**, A124.